Classification of Vehicles using Magnetic Dipole Model

Prateek G V*, Rajkumar V†, Nijil K*, and K.V.S. Hari*

*Statistical Signal Processing Lab
Department of Electrical and Communication Engineering
Indian Institute of Science, Bangalore, India 560012
†Texas Instruments, Bangalore, India
Email: prateekgv@ece.iisc.ernet.in, rajkumarv@ti.com, {nijil,hari}@ece.iisc.ernet.in

***Abstract*—This paper presents an efficient approach to the modeling and classification of vehicles using the magnetic signature of the vehicle. A database was created using the magnetic signature collected over a wide range of vehicles(cars). A vehicle is modeled as an array of magnetic dipoles. The strength of the magnetic dipole and the separation between the magnetic dipoles varies for different vehicles and is dependent on the metallic composition and configuration of the vehicle. Based on the magnetic dipole data model, we present a novel method to extract a feature vector from the magnetic signature. In the classification of vehicles, a linear support vector machine configuration is used to classify the vehicles based on the obtained feature vectors.**

I. Introduction

The data collected by urban planning and development bodies [1] reveal that a great deal of resources are wasted because of the road traffic congestion. The number of man hours wasted due to traffic delay and the amount of pollution are significantly huge. Therefore, there is a great demand for intelligent traffic systems which are capable of monitoring traffic to reduce delay and to smoothen the flow of vehicles. An important parameter of current traffic management systems is the task of vehicle detection and classification. Distinction between different classes of vehicles provides useful information about traffic statistics.

Current technologies that are used in the study of traffic statistics include Intrusive technologies such as Inductive loop [2], Pneumatic tube [3], Piezoelectric [2] [3], Weight-In-Motion [4] and Non-Intrusive technologies such as Microwave Radar [5], Infrared based systems [3], Video-Image processing [6] [7] [8] [9], Passive acoustic system [10]. Amoung all the technologies Induction loop and Video-Image are most widely used but they have a lot of disadvantages. The Induction loop sensor is big in size which makes it difficulty in maintenance and the Video-Image based sensors are costly with big influence of external light conditions. For maximizing the benefits from all these technologies, there must be a large scale deployment of these sensors on all major freeways and local streets.

This project is funded by DIT-ASTeC Wireless Sensor Project, Department of Information Technology, Ministry of Communications & Information Technology, Govt. of India.

Wireless Sensor Networks have a high level of flexibility in their deployment configuration. Since the sensor nodes can be placed virtually anywhere on the road as long as they are within communication range, customized configurations can be adopted for different applications and environments. This unique characteristic is a big advantage over all other surveillance technologies. These passive sensors are mounted on low power consuming wireless transceivers called motes, capable of communicating with each other and a basestation. The sensors are also capable of sensing the magnetic field. Therefore, the field induced due to a large permeable object, like a vehicle, can be sensed. Different vehicles have different metallic components and configuration, which cause different perturbation curves in the presence of a homogeneous magnetic field. This allows us to extract unique characteristics from the recorded magnetic signature. By feeding these attributes to a Support Vector Machine (SVM) [11], the vehicle class [12] can be determined. This can be used as an information for design of automatic toll collection system, prediction of highway capacity, giving signal priority in traffic control system and pavement life estimation in pavement design.

Notation: Bold lower-case alphabets and alphabets with an arrow on top of them represent vectors. Alphabets mentioned in parentheses as a super-script represent the axis direction and are always lower-case letters. Alphabets mentioned as a sub-script represent time-stamp and are always lower-case letters. All upper-case alphabets mentioned represent constants.

In Section II, we present a sensor independent model for modeling the magnetic signature. Based on this model, we propose an algorithm to extract the feature vector in Section III. The obtained feature vector is given to a linear SVM and the performance of the existing and proposed algorithms are studied in Section IV . Conclusions can be found in Section V.

II. Data Modeling

A. Data Collection

The magnetometer senses the magnetic signature of a vehicle whenever the flux lines associated with it is perturbed by a vehicle in its vicinity. HMC1502 [13] is a dual-axis anisotropic magnetoresistance (AMR) [14] magnetometer. It is mounted on a TelosB [15] mote and together they constitute the magnetometer setup. The orientation of the magnetometer is such that it records the Y and Z-axis components of the magnetic field.

Extensive data was collected over a wide range of vehicles. Table I lists out all the cars covered during the data collection and are grouped based on the length of the car. A total of 234 magnetic field readings in Y and Z-axis direction each, were captured. In later sections we will be using Table I to study the performance of the SVM classifier by varying the number of datasets used in training and testing the classifier.

TABLE I
VEHICLE MAGNETIC SIGNATURE DATABASE [16] GROUPED BASED ON THE LENGTH OF THE CAR

Car-type	Type 1	Type 2	Type 3	Type 4
Car Len. (in *meters*)	(3.0-3.5)	(3.5-4.0)	(4.0-4.5)	(>4.5)
Type of *Car(n), where n represents number of datasets Cars = 42 Sets = 89	[1]800(8) [1]Alto(2) [2]Matiz(3) [3]Santro(5) [1]Omni(6) [9]Spark(1) [4]Nano(2) [1]WagonR(4) [1]Estillo(3) [9]Beat(2) [13]Reva(1)	[11]Corsa(2) [3]i20(1) [5]Figo(2) [3]GetZ(2) [3]i10(4) [4]Indica(6) [7]Palio(1) [1]Swift(2) [1]Zen(2) [3]Ritz(1)	[3]Accent(1) [2]Cielo(1) [6]City(4) [12]Vento(1) [1]SX4(2) [3]Verna(1) [1]Esteem(2) [4]Indigo(2) [1]Dzire(1) [4]Sumo(1) [5]Fiesta(1) [6]Petra(1) [14]Logan(1)	[6]Civic(1) [8]Corolla(1) [3]Elentra(2) [8]Innova(2) [7]Linea(1) [3]Sonata(1) [10]Octiva(1) [10]Laura(1)
Number of Datasets	87	67	53	27

* Indicates the Car Manufacturer
[1] - Maruti Suzuki; [2] - Daewoo; [3] - Hyundai; [4] - Tata Motors; [5] - Ford; [6] - Honda; [7] - Fiat; [8] - Toyota; [9] - Chevrolet; [10] - Skoda; [11] - Opel; [12] - Volkswagon; [13] - Mahindra; [14] - Renault.

B. Sensor Independent Model: Magnetic Dipole Model (MDM) [17]

If the distance from the object is large in comparison with its characteristic length, the induced magnetic field $\vec{B}(\mathbf{r},\mathbf{m})$ at position $\mathbf{r} = [x, y, z]^T$ relative to the object can be described as a magnetic dipole field, where $\mathbf{m} = [m^{(x)}, m^{(y)}, m^{(z)}]^T$ is the magnetic dipole moment. An expression of this field $\vec{B}(\mathbf{r},\mathbf{m}) = [B^{(x)}(\mathbf{r},\mathbf{m}), B^{(y)}(\mathbf{r},\mathbf{m}), B^{(z)}(\mathbf{r},\mathbf{m})]^T$ can be derived from Maxwell's equations [18]

$$\vec{B}(\mathbf{r},\mathbf{m}) = \frac{\mu_0}{4\pi}\frac{3(\mathbf{r}\cdot\mathbf{m})\mathbf{r} - r^2\mathbf{m}}{r^5} \tag{1}$$

where $r = \|\mathbf{r}\|_2$ is the L^2-Norm and $(\mathbf{r}\cdot\mathbf{m})$ is the scalar dot product of the two vectors. Substituting $\mathbf{r}$ and $\mathbf{m}$ in equation (1) gives the following

$$B^{(x)}(\mathbf{r},\mathbf{m}) = \frac{\mu_0}{4\pi}\frac{(3x^2 - r^2)m^{(x)} + 3xym^{(y)} + 3xzm^{(z)}}{r^5} \tag{2}$$

$$B^{(y)}(\mathbf{r},\mathbf{m}) = \frac{\mu_0}{4\pi}\frac{3yxm^{(x)} + (3y^2 - r^2)m^{(y)} + 3yzm^{(z)}}{r^5} \tag{3}$$

$$B^{(z)}(\mathbf{r},\mathbf{m}) = \frac{\mu_0}{4\pi}\frac{3zxm^{(x)} + 3zym^{(y)} + (3z^2 - r^2)m^{(z)}}{r^5} \tag{4}$$

The magnetic field at time-instant kT_s is,

$$\vec{B}(\mathbf{r}_k,\mathbf{m}_k) = \begin{bmatrix} B^{(x)}(\mathbf{r}_k,\mathbf{m}_k) \\ B^{(y)}(\mathbf{r}_k,\mathbf{m}_k) \\ B^{(z)}(\mathbf{r}_k,\mathbf{m}_k) \end{bmatrix} \tag{5}$$

where $\mathbf{r}_k = [x_k, y_k, z_k]^T$ is the position vector, $\mathbf{m}_k = [m_k^{(x)}, m_k^{(y)}, m_k^{(z)}]^T$ is the magnetic dipole moments at k^{th} time-instant. Let f be a non-linear function which maps the inputs $\mathbf{r}_k$ and $\mathbf{m}_k$ to $\vec{B}(\mathbf{r}_k,\mathbf{m}_k)$. Let $\mathbf{y}_k$ be the measured output and $\mathbf{e}_k$ be the measurement noise at k^{th} time instant. Then, in the signal processing framework, a sensor can be modeled as a time-invariant system as seen in equation (6).

$$\begin{aligned} \mathbf{y}_k &= f(\mathbf{r}_k,\mathbf{m}_k) + \mathbf{e}_k \\ &= \frac{\mu_0}{4\pi}\frac{3(\mathbf{r}_k\cdot\mathbf{m}_k)\mathbf{r}_k - r_k^2\mathbf{m}_k}{r_k^5} + \mathbf{e}_k \end{aligned} \tag{6}$$

where, $r_k = \|\mathbf{r}_k\|_2$.

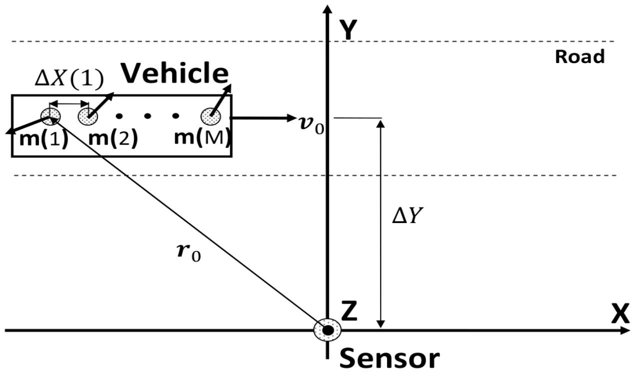

Fig. 1. Illustration of a Magnetic Dipole Model for a Vehicle. $\mathbf{m}(i)$ where, $i \in \{1,\ldots,M\}$ represents magnetic dipole moments, $\Delta X(j)$ where, $j \in \{1,\ldots,M-1\}$ is the separation between adjacent dipoles, ΔY and ΔZ are the offsets, $\mathbf{v}_0$ be the velocity of the vehicle and $\mathbf{r}_0$ be distance of $\mathbf{m}(1)$ from the sensor placed at the origin.

A vehicle can be modeled as an array of magnetic dipoles. The magnetic dipoles are assumed to be located along the longitudinal axis of the vehicle and at a height ΔZ. The vehicle is assumed to move parallel to the X-axis at a certain offset ΔY along the Y-axis and with a constant velocity $\mathbf{v}_0$ (as shown in Fig. 1). We assume that all vehicles in our experiment to pass the sensor with constant velocity. Since the earth's magnetic field is *almost* constant, we can assume that the magnetic dipole moments are constant i.e., $\mathbf{v}_{k+1} = \mathbf{v}_k = \mathbf{v}_0$ and $\mathbf{m}_{k+1} = \mathbf{m}_k = \mathbf{m}$. Also $\mathbf{r}_{k+1} = \mathbf{r}_k + T_s\mathbf{v}_0$. This gives,

$$f(\mathbf{r}_k,\mathbf{m}_k) = f(\mathbf{r}_0 + kT_s\mathbf{v}_0,\mathbf{m}) \tag{7}$$

In general, for an M-Dipole Model, let

- $\mathbf{m}(i) = [m^{(x)}(i), m^{(y)}(i), m^{(z)}(i)]^T$ where, $i \in \{1,\ldots,M\}$ be the magnetic moment of the i^{th} magnetic dipole.
- $\Delta X(j)$ where, $j \in \{1,\ldots,M-1\}$ be the separation between two adjacent magnetic dipoles.
- ΔY and ΔZ be the offsets from Y and Z-axis respectively.

- $\mathbf{v}_0$ the initial velocity and $\mathbf{r}_0$ the initial position

So, the number of parameters to be estimated for an M-dipole model (as shown in Fig. 1) is $4M+1$, assuming the initial velocity of the car and initial position are known. Let $\mathbf{p}$ be the vector of parameters to be estimated, then

$$\begin{aligned} \mathbf{p} &= [\mathbf{m}(i)^T, \Delta X(j), \Delta Y, \Delta Z]^T \\ & \quad \text{where, i} \in \{1, \dots, M\}, \text{j} \in \{1, \dots, M-1\} \end{aligned}$$

Since the vehicle is assumed to move parallel to the X-axis, the only time varying component in $\mathbf{r}_k$ is x_k, that is the component in X-axis direction at k^{th} time instance. Hence,

$$f(\mathbf{r}_k, \mathbf{m}_k) = f(x_k, \mathbf{p}) \tag{8}$$

Let $\hat{\mathbf{p}}$ be the estimate of $\mathbf{p}$. Then, the Non-linear Least Squares (NLS) cost function gives the following

$$\hat{\mathbf{p}} = \arg\min_{\mathbf{p}} V(\mathbf{p}) \tag{9}$$

$$\text{where, } V(\mathbf{p}) = \sum_{k=1}^{N} [\mathbf{y}_k - f(x_k, \mathbf{p})]^T [\mathbf{y}_k - f(x_k, \mathbf{p})]$$

The performance of the MDM for different values of M is seen in Section IV.

III. Feature Extraction

Vehicle Classification is the process of assigning each vehicle into a pre-defined vehicle class based on some features extracted from its magnetic signature. The feature vector is obtained by processing the obtained magnetic signature. First, we will briefly discuss the existing algorithms like Average-Bar Transform [19] and Hill-Pattern Transform [19]. Then, we propose a feature extraction algorithm based on the complexity and the type of the magnetic dipole model called as the Magnetic Dipole Moments and Dipole Separation Algorithm (MDMS Algorithm).

A. Average-Bar Transform [19]

Here the vehicle magnetic signature vector of length N, is divided into S sub-vectors. The mean value of each sub-vector is calculated and the obtained values for S sub-vector is the feature vector. The value of S is fixed for all classes of vehicles. The Z-axis measurements of the magnetometer are primarily used for feature extraction because of their localized character (perturbations in the magnetic field in presence of a vehicle are significant in Z-axis direction).

B. Hill-Pattern Transform [19]

This method transforms the signal into a sequence of $\{+1, -1\}$ and without losing much information. This extracts the pattern of "peaks" and "valleys" (local maxima and minima) of the input signal. The sequence of $\{+1, -1\}$ is used as a feature vector. In this case also the Z-axis measurements of the magnetometer are primarily used for feature extraction.

C. Proposed Algorithm: Magnetic Dipole Moments and Dipole Separation Algorithm (MDMS Algorithm)

We make use of the MDM data model explained in section II-B in this algorithm. The MATLAB [20] function **lsqcurvefit** is used to solve the NLS problem with initial velocity and initial position as an input. The function **lsqcurvefit** returns the estimated parameter vector and the value of the squared 2-norm of the residual at each x_k. The initial velocity and the initial position that give the least residual value of the cost function are picked and based on these values, the parameter vector $\hat{\mathbf{p}}$ is obtained. For every dataset, we also obtain the Root Mean Square Error ($RMSE$) value of the magnetic signature. The $RMSE$ is calculated based on the following equation

$$(RMSE)^2 = \frac{1}{N} \sum_{k=1}^{N} [\mathbf{y}_k - f(x_k, \hat{\mathbf{p}})]^T [\mathbf{y}_k - f(x_k, \hat{\mathbf{p}},)] \tag{10}$$

Curve fitting plots for an M-dipole model where $M \in \{1, 2, 3, 4\}$ of a Tata Indica car using MDMS algorithm is shown in Fig. 2. The initial velocity was assumed to be $1m/s$. From the plots shown in Fig. 2, we observe, as the number of dipoles increases, the curve fits closely or has less curve fitting error.

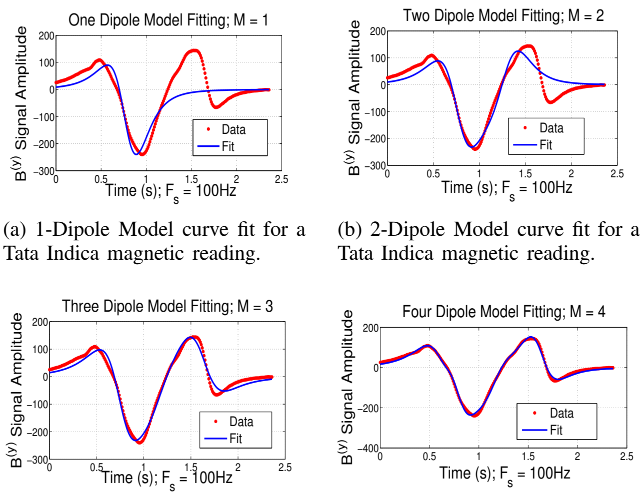

(a) 1-Dipole Model curve fit for a Tata Indica magnetic reading.

(b) 2-Dipole Model curve fit for a Tata Indica magnetic reading.

(c) 3-Dipole Model curve fit for a Tata Indica magnetic reading.

(d) 4-Dipole Model curve fit for a Tata Indica magnetic reading.

Fig. 2. Sample curve fitting plots for measurements corresponding to a Tata Indica car using MDMS algorithm. $M \in \{1, 2, 3, 4\}$. Sampling Frequency, $F_s = 100Hz$. The error in the fit decreases as number of dipoles increases. Location: IISc Campus

Table II shows the obtained parameter values for an M-dipole model where $M \in \{1, 2, 3, 4\}$ and its corresponding $RMSE$ value. Based on the obtained $RMSE$ values, it can be said that, as the number of dipoles increases, the error in the curve fitting decreases.

In order to check the variation of $RMSE$ as the number of dipoles M increases, we calculate the average $RMSE$ for all the datasets mentioned in Table I across different values of $M \in \{1, 2, 3, 4\}$. Let D be the total number of datasets

TABLE II
M-DIPOLE MODEL WITH DIPOLE SEPARATION, DIPOLE MOMENTS AND RMSE FOR A TATA INDICA CAR'S MAGNETIC SIGNATURE

M-Dipole	$\Delta X(j)$	$\tilde{\mathbf{m}}(i) = \frac{\mathbf{m}(i)}{\|\mathbf{m}(i)\|_2}$	$RMSE$
1-Dipole	NA	$\tilde{\mathbf{m}}(1) = (-0.83, -0.09, -0.54)$	67.4
2-Dipole	0.528	$\tilde{\mathbf{m}}(1) = (+0.79, +0.16, +0.58)$ $\tilde{\mathbf{m}}(2) = (-0.80, +0.01, -0.59)$	42.5
3-Dipole	0.474 0.370	$\tilde{\mathbf{m}}(1) = (-0.77, +0.33, -0.52)$ $\tilde{\mathbf{m}}(2) = (+0.26, -0.18, +0.94)$ $\tilde{\mathbf{m}}(3) = (-0.71, -0.19, -0.67)$	19.5
4-Dipole	0.471 0.434 0.001	$\tilde{\mathbf{m}}(1) = (+0.79, +0.29, -0.52)$ $\tilde{\mathbf{m}}(2) = (-0.43, -0.06, +0.89)$ $\tilde{\mathbf{m}}(3) = (+0.35, +0.93, -0.05)$ $\tilde{\mathbf{m}}(4) = (-0.34, -0.93, +0.04)$	12.2

available ($D = 234$, refer Table I) and $RMSE_i$ be the $RMSE$ value for the i^{th} dataset, then the Average $RMSE$ denoted by $\overline{RMSE}$ is computed as follows.

$$\overline{RMSE} = \frac{1}{D}\sum_{i=1}^{D} RMSE_i \tag{11}$$

Table III clearly shows that as the number of magnetic dipoles increases, the $\overline{RMSE}$ decreases. A 4-Dipole Model has the least $\overline{RMSE}$, but it is computationally very complex using the NLS cost function. The computational complexity of the NLS cost function using MATLAB function **lsqcurvefit** is $O\{(4M+1)^3\}$. As the number of dipoles increases by 1, the number of parameters to be estimated increases by 4 and so does the complexity. Also, the decrease in the $\overline{RMSE}$ value is not significantly very sharp as the value of M increases. Ideally on a wireless sensor node one would want to expend minimum energy on computation, so as to increase the longevity of the battery. In the next section, we study the performance of a 3-Dipole Model (3-DM) and a 4-Dipole Model (4-DM) based on the obtained feature vector.

TABLE III
$\overline{RMSE}$ AND NUMBER OF PARAMETERS FOR AVAILABLE DATASETS

M-Dipole Model	Size of $\mathbf{p} = (4M+1)\times 1$	$\overline{RMSE}$
1-Dipole	5×1	17.11
2-Dipole	9×1	10.48
3-Dipole	13×1	7.64
4-Dipole	17×1	5.57

IV. CLASSIFICATION PERFORMANCE

In this section we look at classification of the vehicles mentioned in Table I based on the features obtained using MDMS algorithm. A SVM model usually involves separating data into sets - training and testing. It is built using the datasets that are used as training data. We are using SVM [11] for data classification. Each instance in a training set contains one label value and several attributes. The goal of the SVM is to produce a model (based on the training samples) which predicts the target label of the test sample given only the test sample attributes. Given a training set of instance-label pairs $(\mathbf{x}_i, s_i)$, $i = \{1,\ldots,F\}$ where $\mathbf{x}_i \in \mathbb{R}^P$, $\mathbf{s} \in \{1,-1\}^F$ and

Algorithm 1 Magnetic Dipole Moments and Dipole Separation Algorithm (MDMS Algorithm)

Input: Smoothed Vehicle Magnetic Signature - $\mathbf{a}_{N\times 1}$
Input: The number of magnetic dipoles - M

1: Subtract every $k^{th}, k \in \{1,\ldots,N\}$ sample with the mean of first $N/10$ samples of $a_{N\times 1}$
2: Get the Data Model $\mathbf{a}_k = f(\mathbf{r}_k, \mathbf{m}_k) + \mathbf{e}_k$, as explained in Equation (6)
3: $V(\mathbf{p}) = \sum_{k=1}^{N} [\mathbf{a}_k - f(x_k,\mathbf{p})]^T [\mathbf{a}_k - f(x_k,\mathbf{p})]$, $\mathbf{p}$ be the parameters to estimated and $\mathbf{p} = [\mathbf{m}(i)^T, \Delta X(j), \Delta Y, \Delta Z]^T$
4: Estimate $\mathbf{p}$, $\hat{\mathbf{p}} = \arg\min_{\mathbf{p}} V(\mathbf{p})$
5: Normalized Magnetic Moments $\tilde{\mathbf{m}}(i) = \frac{\mathbf{m}(i)}{\|\mathbf{m}(i)\|_2}$

Output: Normalized Magnetic Dipole Moments $\tilde{\mathbf{m}}(i)$, $i \in \{1,\ldots,M\}$; Separation between adjacent dipoles $\Delta X(j)$, $j \in \{1,\ldots,M-1\}$ and $RMSE$

P is the length of the feature vector then, SVMs require the solution of the following optimization problem

$$\begin{aligned} \min_{\mathbf{w},\gamma,\boldsymbol{\xi}} \quad & \frac{1}{2}\mathbf{w}^T\mathbf{w} + C\sum_{i=1}^{F}\xi_i \\ \text{subject to} \quad & s_i(\mathbf{w}^T\Phi(\mathbf{x}_i)+\gamma) \geq 1-\xi_i, \\ & \xi_i \geq 0. \end{aligned} \tag{12}$$

The function Φ maps the training vectors into a higher dimensional space. SVM finds a linear separating decision hyperplane with the maximal margin in the higher dimensional space. $C > 0$ is the penalty parameter for the error term $\boldsymbol{\xi}$ with i^{th} element ξ_i. Furthermore, $K(\mathbf{x}_i,\mathbf{x}_j) \equiv \Phi(\mathbf{x}_i)^T\Phi(\mathbf{x}_j)$ is called the Kernel function. We used the MATLAB [20] function **svmtrain** to train SVM classifier. To classify new data with the result of the training data, MATLAB function **svmclassify**, which is a binary classifier, is used. In order to randomly pick training and testing data of lengths L_{tr} and L_{ts} respectively, MATLAB function **crossvalind** is used. This function takes in a parameter $q \in [0,1]$ as input which is used to control the lengths of training and testing data. In all our simulation results, we have considered a *linear kernel* function as it performed better than other kernel functions like polynomial kernel, Gaussian radial basis function kernel and hyperbolic tangent kernel.

If Ω_i is the number of vehicles classified correctly among L_{ts} number of cars in the i^{th} iteration and the total number of iterations is I, then using the SVM toolbox functions, the correct rate of classification, C_R across two different classes fixing the training data and testing data lengths is calculated as follows.

$$C_R = \frac{1}{I}\sum_{i=1}^{I}\frac{\Omega_i}{L_{ts}} \tag{13}$$

As the $\overline{RMSE}$ for a 2-Dipole Model and 1-Dipole Model are high compared with 3-Dipole and 4-Dipole Model and the computational complexity of a dipole model for $M > 4$ is high, we compare the performance of MDMS algorithm for a 3-Dipole Model and a 4-Dipole Model using a SVM classifier with a linear kernel function. The value of $I = 100$ is fixed in all our simulations and based on the C_R values obtained, the SVM performance for a 3-Dipole Model and a 4-Dipole Model are compared. We have considered three possible feature vectors in our MDMS algorithm and calculated C_R for different lengths of training and testing datasets of cars belonging to Type 1 (length of the car lies between $3.0m$ to 3.05) and Type 4 (length of the car lies above $4.5m$) category (cars whose lengths are significantly different). In the first case, the estimated normalized magnetic dipole moments is used as a feature vector. In the second case, the estimated separation length between the adjacent dipoles is used as a feature vector and in the third case both the estimated normalized magnetic moments and estimated dipole separation between adjacent dipoles is used as a feature vector to the SVM classifier. From Table IV, the C_R is highest for a 3-Dipole Model with estimated separation between adjacent dipoles as an attribute, followed by a 3-Dipole Model with estimated normalized magnetic moments as an attribute to the SVM classifier.

TABLE IV
RATE OF CLASSIFICATION C_R FOR TYPE 1 VS TYPE 4 CAR BASED ON MDMS ALGORITHM

Dataset Length	Attributes of the SVM Classifier					
	$\tilde{\mathbf{m}}$		ΔX		$\tilde{\mathbf{m}}$ & ΔX	
(L_{tr}, L_{ts})	3-DM	4-DM	3-DM	4-DM	3-DM	4-DM
(60,54)	73.52	71.85	74.25	73.11	71.21	70.04
(65,49)	74.31	72.06	74.60	73.06	72.33	69.71
(70,44)	73.80	73.30	74.14	74.33	71.77	72.23
(75,39)	72.70	73.33	73.29	74.26	70.37	73.11
(80,34)	74.12	73.58	74.27	74.30	72.79	73.15
(85,29)	76.40	74.76	76.61	75.46	74.64	73.21
(90,24)	76.67	75.30	76.78	75.91	75.39	74.52

We compare the performance of MDMS algorithm with the existing algorithms. Table V gives the C_R for different lengths of training and testing datasets of cars belonging to Type 1 (length of the car lies between $3.0m$ to $3.5m$) and Type 4 (length of the car lies above $4.5m$) category. Based on the C_R values obtained, the MDMS algorithm performs better than the Average Bar transform and as good as the Hill-Pattern transform.

Table VI shows the C_R for Type 2 (length of the car lies between $3.5m$ to $4.0m$) and Type 3 (length of the car lies between $4.0m$ to $4.5m$) cars. Based on the C_R values obtained, the MDMS algorithm for a 3-Dipole Model performs better than any other algorithm. The MDMS algorithm gave 75.4% as the correct rate of classification for $(L_{tr}, L_{ts}) = (85, 35)$.

TABLE V
PERCENTAGE OF CORRECT RATE OF CLASSIFICATION C_R FOR TYPE 1 VS TYPE 4 CAR FOR AVERAGE BAR, HILL TRANSFORM AND MDMS ALGORITHM

Datasets	Feature Extraction Algorithms			
(L_{tr}, L_{ts})	Average Bar Algorithm	Hill Transform Algorithm	MDMS Algorithm	
			3-DM $\tilde{\mathbf{m}}$	3-DM ΔX
(60,54)	72.00	76.49	73.52	74.25
(65,49)	73.46	76.67	74.31	74.60
(70,44)	72.70	76.33	73.80	74.14
(75,39)	73.42	75.32	72.70	73.29
(80,34)	73.88	75.39	74.12	74.27
(85,29)	75.36	78.43	76.40	76.61
(90,24)	76.26	77.91	76.67	76.78

TABLE VI
PERCENTAGE OF CORRECT RATE OF CLASSIFICATION C_R FOR TYPE 2 VS TYPE 3 CAR FOR AVERAGE BAR, HILL TRANSFORM AND MDMS ALGORITHM

Datasets	Feature Extraction Algorithms			
(L_{tr}, L_{ts})	Average Bar Algorithm	Hill Transform Algorithm	MDMS Algorithm	
			3-DM $\tilde{\mathbf{m}}$	3-DM ΔX
(60,60)	56.47	52.47	71.93	72.54
(65,55)	57.19	53.59	73.33	73.76
(70,50)	57.67	52.33	71.99	72.60
(75,45)	56.45	51.59	72.65	73.12
(80,40)	57.54	53.90	73.49	73.45
(85,35)	59.59	53.41	75.42	75.41
(90,30)	58.48	51.03	74.74	74.74

V. CONCLUSION

In this paper, we modeled the magnetic signature of a vehicle as an array of magnetic dipoles located along the longitudinal axis of the vehicle. The moments of these magnetic dipoles and the separation between them is extracted using non linear least squares method. We propose Magnetic Dipole Moments and Dipole Separation (MDMS) algorithm based on this model. The moments and separation parameters are considered as the feature vector and a SVM configuration with linear kernel is applied for classification. Based on the percentage of correct rate of classification obtained for different lengths of training and testing data, the MDMS algorithm performs better than existing feature vector algorithms. The performance of MDMS algorithm for Type 1 and Type 4 (cars whose lengths are significantly different) was comparable with the existing algorithms. But for Type 2 and Type 3 (cars whose lengths are not significantly different), the MDMS algorithm gives an improved performance as compared with the existing algorithms.

REFERENCES

[1] J. Pucher, N. Korattyswaropam, N. Mittal, and N. Ittyerah, "Urban transport crisis in india," *Transport Policy*, vol. 12, no. 3, pp. 185 – 198, 2005. http://www.sciencedirect.com/science/article/pii/S0967070X05000272.

[2] P. T. Martin, Y. Feng, and X. Wang, "Detector technology evaluation," MPC Report 03-154, Department of Civil and Environmental Engineering University of Utah Traffic Lab, Nov 2003. http://www.mountain-plains.org/pubs/html/mpc-03-154.

[3] "A summary of vehicle detection and surveillance technologies used in intelligent transportation systems," the vehicle detector clearinghouse, New Mexico State University, Fall 2000. http://www.fhwa.dot.gov/ohim/tvtw/vdstits.pdf.

[4] A. Safaai-Jazi, S. A. Ardekani, and M. Mehdikhani, "A low-cost fiber optic weigh-in-motion sensor," Strategic Highway Research Program

SHRP-ID/UFR-90-002, National Research Council, Washington, D.C., 1990.
[5] A. Duzdar and G. Kompa, “Applications using a low-cost baseband pulsed microwave radar sensor,” in *Instrumentation and Measurement Technology Conference, 2001. IMTC 2001. Proceedings of the 18th IEEE*, vol. 1, pp. 239 –243 vol.1, may 2001.
[6] L. A. Klein, *Data Requirements and Sensor Technologies for ITS*. Norwood, MA: Artech House, 2001.
[7] S. Mantri and D. Bullock, “A neural network based vehicle detection and tracking system,” in *System Theory, 1995., Proceedings of the Twenty-Seventh Southeastern Symposium on*, pp. 279 –283, mar 1995.
[8] M. C.A., S. Hockaday, D. Need, and S. Taff, “Evaluation of video image processing systems for traffic detection,” Tech. Rep. Record No. 1360, National Research Council, Washington D.C., 1992.
[9] “Integration of machine vision and adaptive control in the fast-trac ivhs program,” 72nd annual meeting, Transportation Research Board.
[10] A. Nooralahiyan, H. Kirby, and D. McKeown, “Vehicle classification by acoustic signature,” *Mathematical and Computer Modelling*, vol. 27, no. 9-11, pp. 205 – 214, 1998.
[11] C. Cortes and V. Vapnik, “Support vector machines,” *Machine Leaming*, vol. 20, pp. 273–297, 1995.
[12] “Federal highway administration - vehicle types.” US Department of Transportation. http://www.fhwa.dot.gov/policy/ohpi/vehclass.htm.
[13] Honeywell International Inc., 12001 Highway 55,Plymouth, MN 55441, *1, 2 and 3 Axis Magnetic Sensors HMC1051/HMC1052/HMC1053*. www.sparkfun.com/datasheets/IC/HMC105X.pdf.
[14] H. Hauser, G. Stangl, W. Fallmann, R. Chabicovsky, and K. Riedling, “Magnetoresistive sensors,” 2000.
[15] EasySen, LLC., 401 North Coquillard Dr., South Bend, IN 46617, *SBT80, Multi-Modality Sensor Board for TelosB wireless motes*, Jan 2008. www.easysen.com/support/SBT80v2/DatasheetSBT80v2.pdf.
[16] A. S. Bhat, A. K. Deshpande, K. G. Deshpande, and K. V. S. Hari, “Vehicle detection and classification using magnetometer - data acquisition,” tech. rep., 2011. http://eprints.iisc.ernet.in/43199/.
[17] N. Wahlstro andm, J. Callmer, and F. Gustafsson, “Magnetometers for tracking metallic targets,” in *Information Fusion (FUSION), 2010 13th Conference on*, pp. 1 –8, july 2010.
[18] D. Halliday, R. Resnick, and J. Walker, *Fundamentals of Physics*. John Wiley and Sons, Inc, 5th ed., 1993.
[19] S.-Y. Cheung and P. Varaiya, “Traffic surveillance by wireless sensor networks,” research note, University of California, Berkeley, Jan 2007. http://www.its.berkeley.edu/publications/UCB/2007/PRR/UCB-ITS-PRR-2007-4.pdf.
[20] MATLAB, *version 7.10.0 (R2010a)*. Natick, Massachusetts: The MathWorks Inc., 2010.